

# OTFS - ORTHOGONAL TIME FREQUENCY SPACE

Alirıza Bilir<sup>#1</sup>, Mert Ceylan<sup>#2</sup>, Mustafa Güler<sup>#3</sup>, Yiğithan Özay<sup>#4</sup>, Ömer Faruk Albayrak<sup>#5</sup>

<sup>#</sup>*Electronic and Communication Department, Yildiz Technical University*

<sup>1</sup>18014125

<sup>2</sup>19014070

<sup>3</sup>19014610

<sup>4</sup>20014099

<sup>5</sup>19014057

**Abstract**— This paper proposes a novel 2D modulation technique called Orthogonal Time Frequency Space (OTFS). OTFS takes information from the Delay-Doppler domain, which describes signal delays and Doppler shifts, and translates it into the familiar time-frequency domain used by existing techniques like OFDM, CDMA, and TDMA. Unlike traditional methods that struggle with fading and time-varying channels, OTFS transforms the channel into a stable and time-independent interaction, revealing the underlying channel structure. This allows all data symbols (QAM) to experience consistent channel conditions, and all channel variations within the Delay-Doppler domain are effectively combined. OTFS achieves high-density pilot packing by performing reference signal multiplexing in the time-independent Delay-Doppler domain, which is critical for Massive MIMO systems. This technique enables approaching the channel's maximum capacity regardless of the Doppler effect. OTFS scales throughput linearly with the number of MIMO antennas, unlocking the full potential of Massive MIMO for achieving significant throughput gains even in challenging 5G deployment scenarios.

**Keywords**— OTFS, Massive MIMO, Pilot Packing, Channel Capacity, Delay-Doppler Domain

## I. INTRODUCTION

4G cellular communications has been widely successful, particularly due to its capability to deliver high data rates to a large user base. The demand for these data rates has largely been fueled by the consumption of wireless video, which accounts for approximately 70% of all cellular traffic [2], with a significant portion of users being stationary (> 70% of all connections occur indoors). In recent years, attention has shifted towards the development of fifth-generation cellular communications [3], which is expected to necessitate new applications beyond high-speed video connections, including Internet of Things (IoT) and high-velocity V2X (vehicle-to-vehicle V2V and vehicle-to-infrastructure V2I) connections.

Given the emergence of these new applications, there arises a natural question regarding whether 5G will benefit from a modulation and multiple access method change akin to previous generation transitions, progressing from analog to digital TDMA, CDMA, and OFDM. While OFDM is known to achieve capacity in frequency-selective channels, its optimality is contingent upon specific assumptions such as knowledge of the channel state information (CSI) at the transmitter, Gaussian modulation

alphabet, long codewords (implying absence of latency constraints), and unlimited receiver complexity. However, many of these assumptions are not met in numerous 5G applications, thus necessitating an investigation into a fundamental redesign of modulation and multiple access for next-generation cellular applications.

This paper introduces Orthogonal Time Frequency Space (OTFS) modulation, a new modulation scheme where each transmitted symbol experiences a nearly constant channel gain even in channels with high Doppler or at high carrier frequencies (mm-wave). Essentially, OTFS conducts modulation in the delay-Doppler domain (also known as the Zak domain [4]), which is inherently suited for transmission over time-varying wireless propagation channels. OTFS effectively transforms the time-varying multipath channel into a two-dimensional channel in the delay-Doppler domain. Through this transformation, coupled with equalization in this domain, all symbols over a transmission frame experience the same channel gain.

Equivalently, OTFS can be seen as modulating each information symbol onto one of a set of two-dimensional (2D) orthogonal basis functions in the time-frequency plane, spanning the bandwidth and time duration of the transmission burst or packet. These spread basis functions, when combined with an appropriate equalizer, allow for the extraction of full channel diversity, resulting in the aforementioned almost-constant channel gain. Typically, this leads to a reduction of the standard deviation of power variations from 4 dB to 0.1 dB.

The Zak representation of signals can be interpreted as a generalization of both the time and frequency representations of signals. Hence, OTFS can be viewed as a generalization of OFDM or TDMA; for instance, it reduces to OFDM if the two-dimensional basis functions are subchannel carriers. Furthermore, OTFS is a generalization of (two-dimensional) CDMA, specifically a generalization of DFT-spread OFDM, where the spreading occurs not only along the frequency axis but also in the time-frequency plane. However, unlike CDMA and OFDM, the set of OTFS basis functions is specifically tailored to combat the dynamics of the time-varying multipath channel.

In summary, OTFS is designed to inherit advantageous properties from OFDM, TDMA, and CDMA. Typical gains are on the order of 2 - 4 dB at 10% packet error rates (PERs), and higher for lower target PERs. The relatively

constant channel gain over all symbol transmissions, a hallmark of OTFS, significantly reduces overhead and complexity associated with physical layer adaptation. It also presents the transport and application layers with a robust slowly varying channel, which is highly desirable when running over TCP/IP [5] and for the delay-sensitive applications envisaged for 5G. Moreover, full diversity enables linear scaling of throughput with the number of antennas, regardless of channel Doppler. Additionally, due to the compact representation of the delay-Doppler channel, OTFS enables dense and flexible packing of reference signals, a key requirement to support the large antenna arrays used in massive MIMO.

#### A. Prior Research

The concept of delay-Doppler representation in signal processing has roots in mathematics and physics, as discussed in earlier works [6]. A thorough tutorial on the Zak transform, a key aspect of this representation, can be found in [4]. The detailed exploration of delay-Doppler representation in time-varying channels was pioneered by Bello [7], while its extension to directional time-varying channels, particularly relevant to multiple-antenna systems, was elaborated in [8], [9], and [10].

Since the 1990s, there have been various proposals advocating for the utilization of time-frequency diversity transmission. References [11], [12] introduced a signal model representing the received signal as a canonical decomposition into delay and Doppler shifted versions of a basis signal, proposing a delay-Doppler RAKE receiver to exploit dispersion in both dimensions. Extensions to the multi-antenna scenario are discussed in [10]. Reference [13] highlights that while a time-frequency Rake receiver doesn't achieve optimal diversity due to lack of optimization on the transmit side, linear precoders designed to attain full diversity order in doubly selective channels are introduced. Training strategies for block precoders are detailed in [14], while guard intervals in the frequency domain are formulated in [15].

These approaches, however, differ from OTFS in that their system designs primarily focus on the time-frequency domain rather than the delay-Doppler domain. Other studies have delved into channel estimation in delay-Doppler channels and examined the impact of imperfect CSI. References [16], [17] propose a basis expansion model employing discrete prolate spheroidal sequences, while [18] demonstrates that imperfect CSI doesn't necessarily reduce the Doppler diversity order. Nevertheless, this paper predominantly assumes perfect knowledge of CSI at the receiver.

A separate line of research has concentrated on time-frequency pulse shape design to minimize dispersion after channel transmission, drawing upon Gabor system theory. While a special case of this is pulse-shaped OFDM, earlier works have explored various optimization criteria for pulse shape, including ISI and ICI suppression [19], maximizing SINR [20], and optimizing spectral efficiency through nonrectangular lattices in the time-frequency domain [21]. These efforts differ from OTFS in that they aim to mitigate

or eliminate ISI and ICI through pulse shape design in the time-frequency domain, while OTFS minimizes cross-interference and achieves full diversity through modulation lattice and pulse shape design in the delay-Doppler domain.

While Gabor system theory aims to create ambiguity functions with a single peak at zero, consistent with the Balian-Lowe theorem, OTFS generates ambiguity functions with a sharper peak at zero, periodically repeating along the lattice. OTFS was initially introduced in [1], inspiring subsequent works by various groups [22]-[25], proposing simplified receiver structures usually based on iterative approaches. Additional discussions on discrete signal modeling, modulator design, and performance analysis can be found in [26], [27], while [28] elaborates on the diversity order achievable with different block coder designs, including OTFS. This paper aims to provide a more comprehensive theoretical development compared to [1], encouraging further exploration of various system attributes by the community.

#### B. Further Discussion

IN THE SUBSEQUENT SECTIONS, we delve deeper into our discussion. In Section II-A, we provide an in-depth examination of the wireless channel, focusing specifically on its delay-Doppler characteristics, which serve as the foundation for OTFS design. Following this, Section II further expands on the theoretical groundwork, offering a comprehensive framework for time-frequency modulation.

Moving forward, Section III elaborates on the intricacies of OTFS modulation, detailing the methodology's alignment with wireless channel characteristics through a dual-step processing approach. Subsequently, we explore the conceptual understanding of OTFS and its diverse applications across various 5G scenarios.

Section V is dedicated to presenting empirical evidence illustrating the performance benefits of OTFS when integrated with equalization techniques. These findings highlight OTFS's superiority over OFDM, particularly in environments characterized by high Doppler frequencies, short packet durations, and the use of MIMO arrays. Finally, the paper is brought to a close with a concise summary and concluding remarks in Section VI.

## II. DELAY-DOPPLER REPRESENTATION OF CHANNELS AND SIGNALS

In this section, we delve into the delay-Doppler representation of channels and signals, accompanied by a comprehensive mathematical framework for modulation/demodulation in the time-frequency domain. The insights gained here will serve as the groundwork for the subsequent discussion in Section III, where we provide a detailed exposition of OTFS and establish its relationship with other modulation formats.

#### A. The Delay-Doppler Channel

Since Bello's seminal paper [7], it has been widely recognized that a time-varying propagation channel can be represented by its time-varying impulse response, the time-varying transfer function, or the Doppler-variant

impulse response. Among these representations, the Doppler-variant impulse response is particularly well-suited to capture the physics of propagation. Specifically, the complex baseband Doppler-variant impulse response  $h_c(\tau, \nu)$  characterizes the channel's response to an impulse at delay  $\tau$  and Doppler  $\nu$  [29].

The received signal resulting from an input signal  $s(t)$  transmitted over this channel can be expressed as:

$$r(t) = \iint h_c(\tau, \nu) e^{j2\pi\nu(t-\tau)} s(t-\tau) d\tau d\nu \quad (1)$$

According to this expression, the received signal is a summation of reflected copies of the transmitted signal, each delayed by the path delay  $\tau$ , frequency-shifted by the Doppler shift  $\nu$ , and weighted by the time-independent complex-valued delay-Doppler impulse response  $h_c(\tau, \nu)$  for that particular  $\tau$  and  $\nu$ .

The typical Doppler shifts range from 10 Hz to 1 kHz, although larger values may occur in scenarios involving extremely high mobility (e.g., high-speed trains) and/or high carrier frequencies.

It's worth noting that there are two different interpretations of the Doppler-variant impulse response, which differ by a term  $e^{j2\pi\nu\tau}$ . This difference can be understood as whether we apply the delay shift first and then the Doppler shift, or vice versa. However, as long as the notation remains consistent, equivalent results can be obtained with either definition. This issue is analogous to definitions of the time-varying impulse response, which can either be the response of a system to a delta pulse at time  $t$  or at time  $t-\tau$  [30].

Another important characteristic of the delay-Doppler channel representation  $h_c(\tau, \nu)$  is its compactness and sparsity. Typically, there are only a small number of physical reflectors with associated Dopplers, requiring far fewer parameters for channel modeling and estimation in the delay-Doppler domain compared to the time-frequency domain. This sparse representation has significant implications for channel estimation/prediction, tracking, and complexity management in high-order MIMO and MU-MIMO systems.

### B. The Heisenberg transform and twisted convolution

Conceptually, Eq. (1) can be interpreted as a linear operator  $\Pi_h(\cdot)$  that is parameterized by the impulse response function  $h = h_c(\tau, \nu)$  and that is operating on the input signal  $s(t)$  to produce the output signal  $r(t)$ , that is:

$$\Pi_h(s): s(t) \mapsto r(t). \quad (2)$$

In the mathematics literature, the operator parameterization  $h \rightarrow \Pi_h$  is called the Heisenberg transform which can be viewed as a non-commutative generalization of the Fourier transform. As we will see below, multi-carrier modulations also utilize the Heisenberg transform on the transmitted symbols, hence the received signal is a composition (cascade) of two Heisenberg transforms, one corresponding to the modulation, and the other corresponding to the channel.

### C. Time-Frequency Modulation

**Time-frequency modulator:** A time-frequency modulator with these components maps the 2D symbol sequence  $X[n, m]$  defined on the lattice  $\Lambda$  to a transmitted

signal  $s(t)$  defined as a superposition of delay-and-modulate operations applied to the transmit pulse  $g_{tx}(t)$ , as follows:

$$s(t) = \sum_{m=0}^{M-1} \sum_{n=0}^{N-1} X[n, m] e^{j2\pi m \Delta f (t-nT)} g_{tx}(t-nT). \quad (3)$$

$$f(\tau, \nu) = \sum_{n=0}^{N-1} \sum_{m=0}^{M-1} h_c(\tau-nT, \nu-m\Delta f) X[n, m] e^{j2\pi(\nu-m\Delta f)nT}. \quad (4)$$

**Time-frequency demodulator:** The sufficient statistic for symbol detection is obtained by matched filtering of the received signal  $r(t)$  with the channel-distorted, information carrying pulses (assuming that the additive channel noise is white and Gaussian). The matched filter first computes the cross-ambiguity function between the received signal  $r(t)$  and the receive pulse shape  $g_{rx}$ . This function is denoted  $A_{g_{rx}, r}(\tau, \nu)$  and is given by:

$$A_{g_{rx}, r}(\tau, \nu) \triangleq \int e^{-j2\pi\nu(t-\tau)} g_{rx}^*(t-\tau) r(t) dt \quad (5)$$

**Time-frequency input-output relation:** We have already established in 5 that the input to the matched filter  $r(t)$  can be expressed as the sum of a noise term  $\tilde{v}(t)$  and a signal term  $\Pi_f(g_{tx}(t))$  obtained as the Heisenberg operator parameterized by the impulse response  $f(\tau, \nu)$  applied to the pulse shape  $g_{tx}(t)$ . Consequently, the output of the matched filter, before sampling, is a sum of terms:

$$Y(t, f) = h_c(\tau, \nu) *_{\sigma} X[n, m] *_{\sigma} A_{g_{rx}, g_{tx}}(\tau, \nu). \quad (6)$$

$$H[n, m] = \iint e^{-j2\pi\nu\tau} h_c(\tau, \nu) e^{-j2\pi(m\Delta f\tau - nT\nu)} d\tau d\nu. \quad (7)$$

## III. OTFS MODULATION

We are now ready to describe OTFS modulation cast in the framework of Sec. II as a time-frequency multi-carrier modulation equipped with additional pre-processing transforming from the delay-Doppler domain to the time-frequency domain.

### Interpretations of OTFS modulation

Before going into the mathematical description of OTFS, we first describe the intuition behind it. OTFS can be described in several equivalent ways:

**Delay-Doppler Domain Modulation:** Similar to how OFDM carries information using compact "basis pulses" in the time-frequency domain, OTFS uses compact basis functions in the delay-Doppler domain. These functions are modulated with QAM symbols to transmit information. While an OFDM waveform interacts with the channel by multiplying the basis pulses with the time-varying transfer function, OTFS interaction involves a two-dimensional convolution of its basis function with the Doppler-variant impulse response (the two-dimensional Fourier dual of the transfer function). This interpretation will be our primary focus for further mathematical derivations.

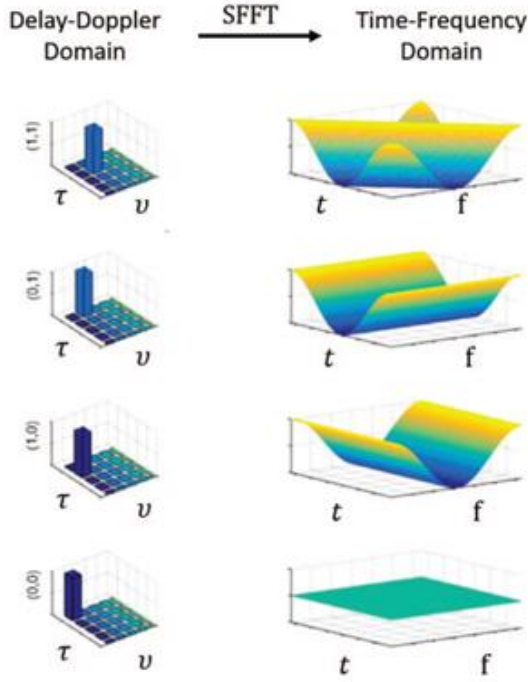


**Figure 1** 2D basis functions in the Information (delay-Doppler) domain (left), and the corresponding symplectic Fourier dual basis functions in the time-frequency domain (right).

**Time-Frequency Domain Spreading:** Another perspective views OTFS as a spreading technique in the time-frequency domain. Information is carried on non-compact (maximally spread) orthogonal basis functions, as shown in Figure 1. In this sense, OTFS resembles a two-dimensional version of CDMA. This interpretation allows for easier analysis of achievable diversity gains.

**Zak Transform Representation:** A more formal description positions OTFS as the natural modulation format associated with the Zak transform, similar to how OFDM is linked to the Fourier transform.

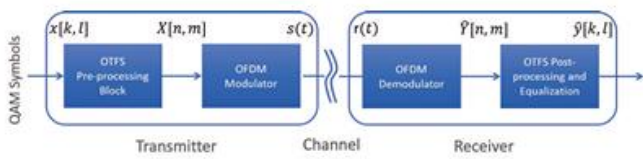


**Figure 2** OTFS Modulation Block Diagram: Transmitter and Receiver

## B. OTFS Modulation and Demodulation

The OTFS modulation process involves two key transformations at both the transmitter and receiver (refer to Figure 2). At the transmitter, the first step maps a 2D sequence of information symbols  $x[k, l]$  residing in specific locations within a mathematical structure called the reciprocal lattice ( $\Lambda_\perp$ ) to the delay-Doppler domain. This is followed by the OTFS transform, which combines the finite symplectic Fourier transform with windowing. This combined operation maps the symbols to a new 2D sequence  $X[n, m]$  located within the time-frequency domain ( $\Lambda$ ). Finally, the Heisenberg transform converts

these time-frequency symbols ( $X[n, m]$ ) into a time domain signal ( $s(t)$ ) suitable for transmission over the channel.

The receiver performs the opposite steps to recover the original information. The received time signal ( $r(t)$ ) is first transformed back into the time-frequency domain using the discrete Wigner transform. Lastly, the inverse finite symplectic Fourier transform maps the recovered symbols back to the delay-Doppler domain, allowing for symbol detection and retrieval of the original information ( $x[k, l]$ ).

In simpler terms, OTFS utilizes a series of mathematical transformations to represent information efficiently. This representation is particularly robust against channel variations, especially in high-mobility scenarios.

**OTFS delay-Doppler modulator:** Consider a finite 2D sequence of QAM information symbols  $x[k, l]$ , where  $k = 0, \dots, M-1$  and  $l = 0, \dots, N-1$  that we wish to transmit. Let us denote by  $x_p[k, l]$  the 2D periodized version of  $x[k, l]$  with periods  $(M, N)$ . Further, let us assume a time-frequency modulation system defined by the lattice, packet burst, and bi-orthogonal transmit and receive pulses as described in Section II-C. In addition, let us assume a square summable transmit windowing function  $W_{tx}[n, m]$  that multiplies the modulation symbols in the time-frequency domain. Given the above components, the OTFS modulated symbols are defined as follows:

$$X[n, m] = W_{tx}[n, m] \text{SFFT}(x_p[k, l]) \quad (8)$$

The transform (8) is comprised of the SFFT followed by a windowing operation in time-frequency and is referred to as the OTFS transform. The transmitted signal is obtained from the modulated sequence using the Heisenberg transform as follows:

$$s(t) = \Pi_X(g_{tx}(t)). \quad (9)$$

The composition of the OTFS transform and the Heisenberg transform comprises the OTFS modulation, as shown in the two transmitter blocks of Fig. 2. An alternative interpretation expresses the output of the OTFS transform in the form:

$$X[n, m] = W_{tx}[n, m] \sum_{k=0}^{M-1} \sum_{l=0}^{N-1} x[k, l] b_{k, l}[n, m], \quad (10)$$

where  $b_{k, l}[n, m]$  is the 2D sequence given by the sampled symplectic Fourier exponential function:

$$b_{k, l}[n, m] = e^{-j2\pi(\frac{mk}{M} - \frac{nl}{N})}. \quad (11)$$

This interpretation of (10) casts the OTFS transform as a CDMA like spreading system in time-frequency. It shows that each information symbol  $x[k, l]$  is modulated by a 2D basis function  $b_{k, l}[n, m]$  in the time-frequency domain, the shape of which is shown in Fig. 1. From this interpretation it is clear that every OTFS QAM symbol is spread over the full time-frequency grid and hence is able to exploit the diversity associated with all the modes of the channel.

**OTFS delay-Doppler demodulator:** For the definition of the demodulator let us assume a square summable receive windowing function  $W_{rx}[n, m]$  and consider a

receive signal  $r(t)$ . The receive signal is demodulated as described in the following four steps:

1) Apply the (discrete) Wigner transform to the signal  $r(t)$  to obtain a time-frequency 2D sequence of demodulated symbols with unbounded support:

$$\hat{Y}[n, m] = A_{g_{rx}, r}(\tau, \nu)|_{\tau=nT, \nu=m\Delta f}. \quad (12)$$

2) Apply the receive window function  $W_{rx}[n, m]$  to the sequence  $\hat{Y}[n, m]$  to obtain a shaped time-frequency 2D sequence of bounded support:

$$\hat{Y}_W[n, m] = W_{rx}[n, m] \hat{Y}[n, m]. \quad (13)$$

3) Periodize the sequence  $\hat{Y}_W[n, m]$  to obtain a periodic time-frequency 2D sequence with periods  $(N, M)$  along time and frequency respectively:

$$\hat{Y}_p[n, m] = \sum_{n'=-\infty}^{\infty} \sum_{m'=-\infty}^{\infty} \hat{Y}_W[n - n'N, m - m'M]. \quad (14)$$

4) Apply the inverse SFFT to the periodic time-frequency sequence  $\hat{Y}_p[n, m]$  to obtain a periodic delay-Doppler sequence:

$$\hat{y}_p[k, l] = \text{SFFT}^{-1}(\hat{Y}_p[n, m]). \quad (15)$$

The output sequence of demodulated symbols is obtained as  $\hat{y}[k, l] = \hat{y}_p[k, l]$  for  $k = 0, \dots, M-1$  and  $l = 0, \dots, N-1$ . The last step can be interpreted as a projection of the timefrequency modulation symbols onto the two-dimensional orthogonal basis functions  $b_{k,l}[n, m]$  as follows:

$$\hat{y}[k, l] = \frac{1}{NM} \sum_{n=0}^{N-1} \sum_{m=0}^{M-1} \hat{Y}_p[n, m] b_{k,l}^*[n, m], \quad (16)$$

where  $b_{k,l}^*[n, m]$  stands for the conjugate 2D basis function:

$$b_{k,l}^*[n, m] = e^{-j2\pi(\frac{kn}{N} - \frac{lm}{M})}. \quad (17)$$

**OTFS delay-Doppler input-output relation:** We conclude this development with a description of the input-output relation between the periodic delay-Doppler modulated and demodulated sequences  $x_p$  and  $\hat{y}_p$  respectively. The relation is roughly given, up to an additive noise term, by convolution with the Doppler variant channel impulse response  $h_c(\tau, \nu)$ . In more precise terms, consider the periodic convolution of the channel impulse response with a filtering function as follows:

$$h_w(\tau, \nu) = \iint e^{-j2\pi\nu\tau'} h_c(\tau', \nu') w(\nu - \nu', \tau - \tau') d\tau' d\nu'. \quad (18)$$

The filtering function  $w(\tau, \nu)$  is a periodic function with periods  $(M\Delta\tau, N\Delta\nu)$  in delay and Doppler respectively, obtained as the inverse discrete symplectic Fourier transform (denoted by SDFT) of a time-frequency window  $W[n, m]$ , that is:

$$w(\tau, \nu) = \sum_{n=-\infty}^{\infty} \sum_{m=-\infty}^{\infty} e^{-j2\pi(\nu nT - \tau m\Delta f)} W[n, m], \quad (19)$$

where  $W[n, m] = W_{tx}[n, m]W_{rx}[n, m]$  is the product of the transmit and receive windows. Note that as the support of

the window  $W[n, m]$  along time and frequency increases, the filtering function  $w$  gets narrower in delay-Doppler and as a result  $h_w(\tau, \nu)$  more closely approximates the true channel impulse response  $h_c(\tau, \nu)$ . The OTFS input-output relation is summarized in the following key theorem.

#### OTFS delay-Doppler input-output relation.

The input-output relation between the periodized demodulated noisy sequence  $\hat{y}_p[k, l]$  and the periodized transmitted information symbol sequence  $x_p[k, l]$  is given by:

$$\hat{y}_p[k, l] = \frac{1}{NM} \sum_{k'=0}^{M-1} \sum_{l'=0}^{N-1} h_w(k' \Delta\tau, l' \Delta\nu) \times x_p[k - k', l - l'] + v_p[k, l], \quad (20)$$

where  $v_p[k, l] = \text{SFFT}^{-1}(V_p[n, m])$  and  $V_p[n, m]$  stands for the periodization of the sampled and windowed time-frequency noise term  $W_{rx}[n, m]V[n, m]$ .

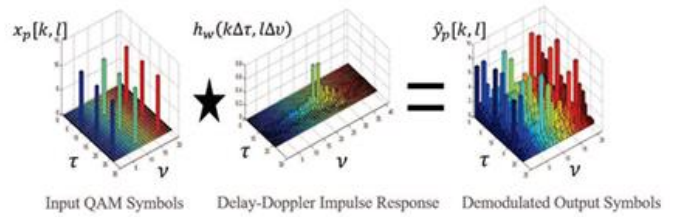


**Figure 3** "Clean" OTFS delay-Doppler input-output relation (in the absence of noise): Convolution of (sampled and filtered) channel delay-Doppler impulse response with modulation symbols in the delay/Doppler domain.

#### C. Equalization

For typical system parameters of broadband transmission, the assumption that the support of the channel impulse response is limited to the neighborhood of a lattice point, and thus the bi-orthogonality condition, is not fulfilled. Consequently, the 2D intersymbol interference (20) must be eliminated by a suitable equalizer. Possible structures include the 2D versions of standard equalizers, namely (i) linear equalizers, (ii) non-linear equalizers such as decision feedback and maximum-likelihood sequence estimators, possibly approximated as turbo equalizers. While a detailed discussion of equalizer structures for OTFS is beyond the scope of this paper, we note that linear equalizers generally perform poorly. The impact of advanced equalizer structures on receiver complexity is limited due to the sparsity and translation invariance of the channel response, and the relative impact on overall receiver complexity (including decoding) is even less pronounced, especially since many modern systems use maximum-likelihood receivers.

### IV. INTERPRETATION AND IMPLEMENTATION

#### A. Implementation as overlay

OTFS can be implemented in a variety of ways. One expedient method is as an overlay of an existing OFDM system, since highly optimized hardware already exists for such systems, especially in the context of cellular (3GPP) and wireless LAN (WiFi) systems. Figure 4 shows the flow diagram that makes use of this structure. Current OFDM



transceivers already implement a form of the Heisenberg/Wigner transform. At the transmitter, it is thus sufficient to perform a 2D OTFS transform (which can be implemented as a 2D SFFT), and let the resulting symbols be the input for the existing OFDM modulator. At the receiver, the output of the (soft) OFDM demodulator also undergoes a 2D OTFS transform, the results of which are used as input to the OTFS equalizer and demodulator. This can be thought of as a generalization of the approach in single-carrier (SC) FDMA (also referred to as DFT-spread-OFDM) where a one-dimensional FFT is applied.

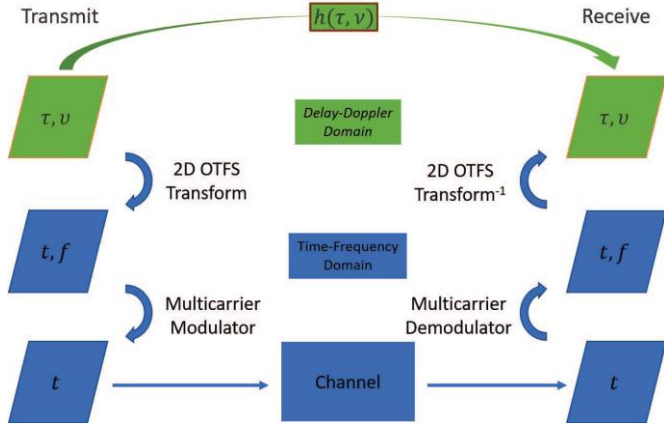


**Fig. 4.** Signal flow in an implementation of OTFS as time-frequency overlay.

In terms of implementation complexity, we have to consider two components: the Heisenberg transform is already implemented in today's systems in the form of OFDM/OFDMA, corresponding to a prototype filter  $g(t)$  which is a square pulse. Other filtered OFDM and filter bank variations have been proposed for 5G [35], which can also be accommodated in this general framework with different choices of  $g(t)$ . The second step of OTFS is the 2D finite symplectic Fourier transform (SFFT). We now compare that complexity to that of SC-FDMA: for a frame of  $N$  OFDM symbols consisting of  $M$  subcarriers each, SC-FDMA adds  $N$  DFTs of  $M$  points each (assuming the worst case that all subcarriers are given to a single user). For these parameters, the additional complexity of SC-FDMA is then  $MN \log_2(M)$  over the baseline OFDM architecture. For OTFS, the 2D SFFT has complexity  $MN \log_2(MN) = MN \log_2(M) + MN \log_2(N)$ , so the term  $MN \log_2(N)$  is the OTFS additional complexity compared to SC-FDMA. For an LTE subframe with  $M = 1200$  subcarriers and  $N = 14$  symbols, the additional complexity is 37% more compared to the additional complexity of SC-FDMA. However, note that this complexity increase only occurs if OTFS is implemented on top of an existing transceiver. Just like for SC-FDMA, some operations of the preprocessing and the IFFT of the OFDM modulator cancel each other out. In fact, one can show that an optimized OTFS transmitter has a complexity that is essentially half of that of an equivalent OFDM transmitter.

## B. Multiplexing

There are a variety of ways to multiplex several uplink or downlink transmissions in one OTFS frame. The most natural one is multiplexing in the delay-Doppler domain, such that different sets of OTFS basis functions, or sets of information symbols or resource blocks are given to different users. Given the orthogonality of the basis functions, the users can be separated at the receiver. For the downlink, the UE (user equipment) need only demodulate the portion of the OTFS frame that is assigned to it. This approach is the natural dual to resource block allocation in OFDMA. It is noteworthy, however, that the OTFS signals from all users extend over the whole time-frequency window, thus providing full diversity; by this we mean that for a channel with  $Q$  clustered reflectors ( $Q$  multipath components separable in either the delay or Doppler dimension) the OTFS modulation can achieve a diversity order equal to  $Q$ .

Furthermore, this full spreading is also advantageous from a Peak to Average Power Ratio (PAPR) point of view (see Sec. IV-D). In the uplink direction, transmissions from different users experience different channel responses. Hence, the different subframes in the OTFS domain will experience a different channel. This can potentially introduce inter-user interference at the edges where two user subframes are adjacent and would require guard gaps to eliminate it. An alternative is multiplexing in the time-frequency domain, i.e., different resource blocks or subframes are allocated to different users. These resource blocks can either be contiguous, or interleaved. In the former case, each user's signal is transmitted over a subset of the time-frequency plane, and thus has reduced diversity.

## C. Diversity and channel gain

From (43) we see that over a given frame, each demodulated symbol  $\hat{x}[k, l]$  for a given  $k$  and  $l$  experiences the same channel gain on the transmitted symbol  $x[k, l]$ . This combined with a non-linear equalizer at the receiver, as discussed in Sec. III-C, allows to extract the full channel diversity. The

almost-constant channel offers several important performance benefits. Firstly, it obviates the need for fast adaptive modulation and coding (AMC). While AMC provides significant benefits in slowly varying channels [36], it might either require high feedback overhead, or be completely impossible (when the channel coherence time

is less than the feedback time) in systems operating in fast-varying channels. If obtaining accurate CSI (channel state information) knowledge at the TX becomes impossible, then channel variations are detrimental to performance, as the AMC must be chosen to accommodate the worst-case SNR. Thus, for high-mobility situations (vehicle-to-vehicle, high-speed train, etc.), channel whitening through spreading, and thus operating with a constant SNR over extended time periods, is not only the simpler solution, but also provides the better performance. The importance of a robust and fixed-rate channel is increased for applications that - due to latency constraints - do not allow retransmissions. This is especially critical for running applications over the TCP/IP protocol, which dramatically backs off the rate when packet failures occur, and subsequently takes a long time to converge again to a higher rate.

A high diversity could also be achieved in OFDM, using suitable interleaving and coding. However, that solution is subject to a number of drawbacks: (i) the information is not uniformly distributed over the time-frequency plane; thus diversity is not fully exploited, and the higher the code rate the more pronounced is the effect; (ii) it is not an effective solution for short codewords, since the diversity is upper bounded by the number of transmitted bits; in contrast OTFS always provides full diversity. A second important advantage of the almost-constant channel lies in enabling simplified equalizers and decoders, as well as precoders. For example, within the duration of an OTFS symbol, the equalizer coefficients do not have to be adapted, while every symbol in OFDM needs a different (though significantly simpler) equalizer.<sup>12</sup> More important, any signal predistortion can be done equally for all signals. The convergence to a constant channel gain can also be interpreted as "channel hardening", an effect well known from massive MIMO systems [37]. Notably, this effect inherently occurs even in a single-antenna OTFS system. This can be explained by interpreting the antenna locations of the UE at different times during the considered time window as a massive "virtual array".

#### D. PAPR

Low PAPR is an important goal for modulation/multiple access design since it reduces the maximum linear power requirements for the transmit amplifiers. This is particularly important for the uplink of cellular systems, since amplifiers in consumer devices such as handsets need to be low-cost. OTFS (considered here with delay/Doppler multiplexing) reduces uplink PAPR in two ways: (i) if a user is assigned a single Doppler frequency, then the PAPR is the same as for single-carrier transmission, i.e., significantly lower than for OFDM. (ii) in conjunction, due to the spreading operation, the packet transmission extends over a longer period of time than in OFDM which allows to increase the maximum energy per bit under Tx power constraints. This is particularly relevant for short packets.

It is noteworthy that especially for short packets, OTFS achieves a superior trade-off between PAPR and performance compared to SC-FDMA, even in time-

invariant channels. While SC-FDMA can have low PAPR during the active signal duration, the overall PAPR is only small if the signal has a duty cycle close to unity, which in turn requires that (due to the small packet size) it utilizes only a single (or very few) subcarriers. However, such an approach, which is also used by LTE, leads to low frequency diversity and thus inferior performance; furthermore, for very short packets, SC-FDMA might still have a duty cycle  $< 1$  even for such a configuration. OTFS, on the other hand, can obtain full spreading in time and frequency while keeping the PAPR low.

Standard SC-FDMA multiplexes data over contiguous bands. A more sophisticated variant is referred to as hopped SC-FDMA. This mode of transmission maximizes the link budget as it enjoys low PAPR comparable to single carrier and maximizes transmission duration, while at the same time extracting additional diversity gain. However, there is a subtle phenomenon that renders this approach sub-optimal. To maintain low PAPR, the QAM order must be kept low - say QPSK. Under this constraint, the transmission rate can only be adjusted by changing the FEC rate, and thus the performance is governed by the restricted QPSK capacity instead of by the Gaussian capacity.

## V. PERFORMANCE RESULTS

In the following we present some results that demonstrate some key benefits of OTFS. The parameters of the simulations are chosen to be comparable to, and consistent with, a use of OTFS as an "overlay" of a 4G LTE system (further advantages could be achieved by the use of an OTFS "greenfield" system, e.g., by abolishing the cyclic prefix as discussed above). Thus, the performance advantages presented here can be seen as a lower bound on the performance gains relative to OFDM.

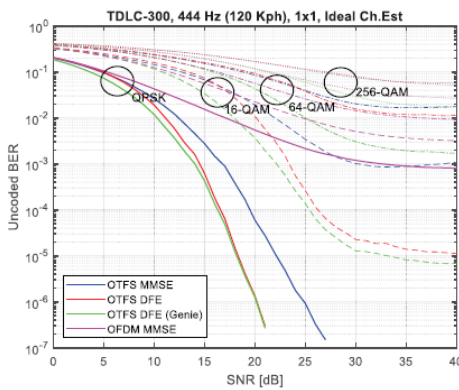
To be more specific, the simulations use the PHY layer parameters to comply with the 4G LTE specification (ETSI TS 36.211 and ETSI TS 36.212), unless otherwise specified. For the OTFS system we add the OTFS transform pre- and post-processing blocks at the transmitter and receiver respectively. We simulate the wireless fading channel according to the TDL-C channel model (delay spread of 300 ns, Rural Macro, and low correlation MIMO), one of the standardized channel models in 3GPP. The details of the simulation parameters used are summarized in Table I.

Figure 5 shows the BER of an uncoded system operating in a time-and-frequency dispersive channel, with a medium

Parameter	Value
Carrier frequency (GHz)	4.0
Duplex mode	FDD
Subcarrier spacing (kHz)	15
Cyclic prefix duration ( $\mu$ s)	4.7
FFT size	1024
Transmission bandwidth (resource blocks)	50
Antenna configuration	1T 1R (SISO)
Rank	Fixed rank
MCS	fixed: 4QAM, 16 QAM, 64 QAM
Control and pilot overhead	none
Channel estimation	ideal
Channel model	TDL-C, DS=300 ns

TABLE I  
SIMULATION PARAMETERS FOR PERFORMANCE RESULTS

Doppler (velocity corresponding to highway vehicle speed) and with different modulation formats. When comparing the results of OFDM modulation to that of OTFS, when both are using MMSE equalizers, we find that for low modulation order (4QAM and 16 QAM), OTFS outperforms OFDM; in particular for 4QAM OFDM shows a significant error floor due to the intercarrier interference that is not present for OTFS. Furthermore, we see that the slope of the BER-vs-SNR curve is steeper for OTFS than for OFDM even outside the "error floor" region, which can be explained by the higher diversity order. However, we also note that for higher-order modulation OFDM outperforms OTFS with MMSE (in line with the discussion in Sec. III.C). This can be remedied by the use of a non-linear equalizer in OTFS. We analyze in particular DFE structures, distinguishing between "standard" DFE and DFE with "genie"-aided feedback (i.e., for the interference subtraction the DFE knows the correct symbol sequence). We see that for 4QAM, there is at most a 1dB difference of the SNR when comparing genie-aided to standard DFE, indicating that error propagation is not a significant issue. However, error propagation can be more significant at higher modulation orders.



**Fig.5.** Uncoded BER for 4QAM/16QAM/64QAM/256QAM, TDL-C channel model, 120kmph. Curves show OFDM with MMSE equalizer, and OTFS with (i) MMSE equalizer, (ii) DFE equalizer with error propagation, and (iii) DFE equalizer with genie feedback.

Figure 6 shows the coded error rate for a variety of equalizer structures. We again compare OFDM with MMSE equalization, to OTFS with MMSE and with DFE. We firstly see that MMSE equalization is not suitable for use in OTFS, and would lead to equal or worse

performance than OFDM. We also see that due to error propagation, the standard DFE does not perform well either. These trends are much more pronounced at low code rate and high modulation order, consistent with our discussion of the uncoded case. However, an iterative DFE (which is seen to closely approximate the performance of a genie-aided DFE) performs very well, and OTFS with such a receiver significantly outperforms OFDM.

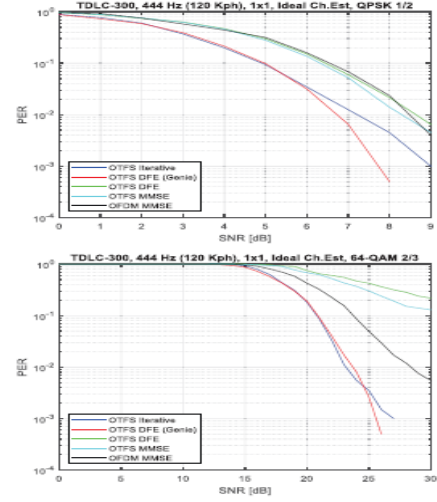


**Fig.6.** BLER for 4QAM, coderate 1/2 and 64QAM coderate

We next simulate a situation with short packets. Figure 7 shows the BLER performance for a system with mobile speeds of 30 km/h if only 4 resource blocks (48 subcarriers), called PRBs in LTE, are occupied by the user of interest out of a total of 50 resource blocks (600 subcarriers). This corresponds to a short packet length. Notice the increased diversity gain of OTFS compared to OFDM in this case resulting in gains of 4 dB or more as SNR increases. This diversity gain is because the OTFS transform spreads each QAM symbol over all time and frequency dimensions of the channel and then extracts the resulting full diversity, while OFDM limits the transmission to a narrow subchannel of 48 subcarriers.

A similar situation arises when a number of users are multiplexed, leading to a smaller percentage of resources for each user. Figure 8 illustrates this effect. It shows the coded.

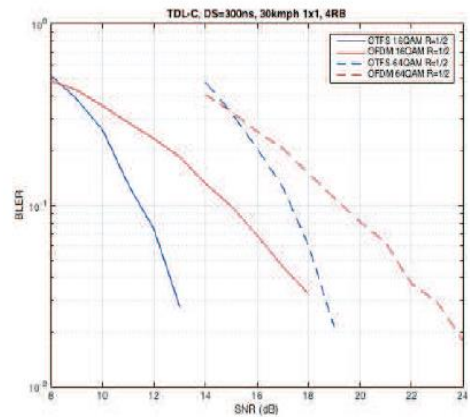




**Fig. 7.** BLER for short packet length (4 PRBs out of 50), 16QAM/64QAM, Code rate  $R=1/2$ , 30kmph.

PER when the packet size per user is varied (corresponding to having to supply a different number of users). For OFDM, performance becomes worse as the packet size decreases, since it implies that the diversity of the system decreases. OTFS shows essentially unchanged behavior for packet sizes ranging from 2 to 50 PRB (physical resource blocks).

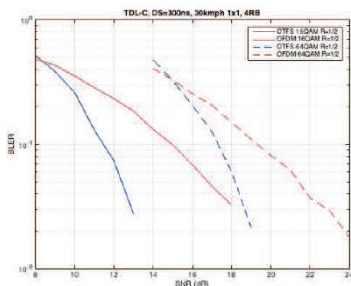


**Fig. 8.** BLER for QPSK with rate 1/2 code and different numbers of users

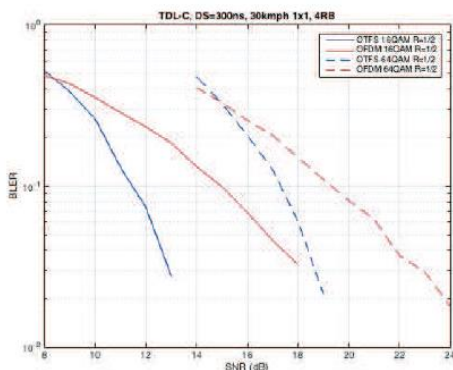


**Fig. 8.** BLER for QPSK with rate 1/2 code and different numbers of users

As pointed out previously, one of the key advantages of OTFS is the stability of the effective SNR, which not only provides better operating points in systems without sufficiently fast CQI feedback, but also offers a more stable channel to the MAC layer. Figure 9 shows an example for this effect. In an ETU channel with 120 km/h UE mobility, the SNR seen by an OFDM system shows significant variations (more than 4 dB standard deviation), while the SNR of an OTFS system with a 1 ms window has only 1.1 dB standard deviation, and OTFS with a 10 ms time window is almost constant (standard deviation 0.2 dB). When considering the cdf of the SNR, if an outage probability of 0.01 is required, then an OFDM system requires a fading margin that is 7 dB larger than OTFS with a 1 ms window, and 9 dB compared to OTFS with a 10 ms window.

## Conclusion

In this paper we developed OTFS, a novel two-dimensional modulation scheme for wireless communications with significant advantages in performance over existing modulation schemes such as TDMA and OFDM. OTFS operates in the delay-Doppler coordinate system and we showed that with this modulation scheme coupled with equalization, all modulated symbols experience the same channel gain by extracting the full channel diversity. As a result of its operating principle, OTFS has the following important advantages: • No need for channel adaptation, since OTFS provides a stable data rate. This is especially important in systems with high mobility, where feedback of CSI to the transmitter becomes impossible, or afflicted with large overhead. • Better packet error rates (for the same SNR) or reduced SNR requirements (for the same PER) in the presence of high mobility (V2V, high-speed rail), or high phase noise (mm-wave systems). • Improved PAPR, in particular for short packet transmission. • Improved MIMO capacity when using finite-complexity receivers. As a new modulation format, there are many aspects of OTFS that merit closer investigation, to optimize performance, reduce complexity, and enhance coexistence with existing systems. These aspects will be investigated in future publications.

## REFERENCES

- S. M. Metev and V. P. Veiko, *Laser Assisted Microtechnology*, 2nd ed., R. M. Osgood, Jr., Ed. Berlin, Germany: Springer-Verlag, 1998.
- J. Breckling, Ed., *The Analysis of Directional Time Series: Applications to Wind Speed and Direction*, ser. Lecture Notes in Statistics. Berlin, Germany: Springer, 1989, vol. 61.
- S. Zhang, C. Zhu, J. K. O. Sin, and P. K. T. Mok, "A novel ultrathin elevated channel low-temperature poly-Si TFT," *IEEE Electron Device Lett.*, vol. 20, pp. 569–571, Nov. 1999.
- M. Wegmuller, J. P. von der Weid, P. Oberson, and N. Gisin, "High resolution fiber distributed measurements with coherent OFDR," in *Proc. ECOC'00*, 2000, paper 11.3.4, p. 109.
- R. E. Sorace, V. S. Reinhardt, and S. A. Vaughn, "High-speed digital-to-RF converter," U.S. Patent 5 668 842, Sept. 16, 1997.
- (2002) The IEEE website. [Online]. Available: <http://www.ieee.org/>
- M. Shell. (2002) IEEEtran homepage on CTAN. [Online]. Available: [http://www.ctan.org/tex-archive/macros/latex/contrib/supported/IEEEtran/FLEXChip Signal Processor \(MC68175/D\), Motorola, 1996.](http://www.ctan.org/tex-archive/macros/latex/contrib/supported/IEEEtran/FLEXChip Signal Processor (MC68175/D), Motorola, 1996.)
- "PDCA12-70 data sheet," Opto Speed SA, Mezzovico, Switzerland.
- A. Karnik, "Performance of TCP congestion control with rate feedback: TCP/ABR and rate adaptive TCP/IP," M. Eng. thesis, Indian Institute of Science, Bangalore, India, Jan. 1999.
- J. Padhye, V. Firoiu, and D. Towsley, "A stochastic model of TCP Reno congestion avoidance and control," Univ. of Massachusetts, Amherst, MA, CMPSCI Tech. Rep. 99-02, 1999.
- Wireless LAN Medium Access Control (MAC) and Physical Layer (PHY) Specification*, IEEE Std. 802.11